

## UvA-DARE (Digital Academic Repository)

### Trapping Atoms in a Dark Optical Lattice

Hemmerich, A.; Weidemuller, M.; Esslinger, T.; Zimmermann, C.; Hansch, T.

DOI

[10.1103/PhysRevLett.75.37](https://doi.org/10.1103/PhysRevLett.75.37)

Publication date

1995

Published in

Physical Review Letters

[Link to publication](#)

#### Citation for published version (APA):

Hemmerich, A., Weidemuller, M., Esslinger, T., Zimmermann, C., & Hansch, T. (1995). Trapping Atoms in a Dark Optical Lattice. *Physical Review Letters*, 75, 37-40. <https://doi.org/10.1103/PhysRevLett.75.37>

#### General rights

It is not permitted to download or to forward/distribute the text or part of it without the consent of the author(s) and/or copyright holder(s), other than for strictly personal, individual use, unless the work is under an open content license (like Creative Commons).

#### Disclaimer/Complaints regulations

If you believe that digital publication of certain material infringes any of your rights or (privacy) interests, please let the Library know, stating your reasons. In case of a legitimate complaint, the Library will make the material inaccessible and/or remove it from the website. Please Ask the Library: <https://uba.uva.nl/en/contact>, or a letter to: Library of the University of Amsterdam, Secretariat, Singel 425, 1012 WP Amsterdam, The Netherlands. You will be contacted as soon as possible.

## Trapping Atoms in a Dark Optical Lattice

A. Hemmerich, M. Weidemüller, T. Esslinger, C. Zimmermann, and T. Hänsch

*Sektion Physik, Universität München, Schellingstraße 4/III, D-80799 Munich, Germany  
and Max-Planck-Institut für Quantenoptik, D-85748 Garching, Germany*

(Received 19 December 1994)

We demonstrate a new type of optical lattice which confines atoms in nearly dark states. The lattice is formed by cooperation of an optical standing wave detuned to the blue with respect to an atomic  $F = 1 \rightarrow F = 1$  transition and a homogeneous magnetic field. The atoms are predominantly localized where the light is purely  $\pi$  polarized such that they are optically pumped to the  $m_F = 0$  Zeeman component which is decoupled from the light field. We have observed quantized vibrations of the localized atoms by means of probe transmission spectroscopy. Our “dark” optical lattice works in two and three dimensions.

PACS numbers: 32.80.Pj, 42.65.-k

In the recent past, optical lattices have received much attention in atomic physics because they represent a unique, unusual state of matter: neutral atoms laser cooled to the microkelvin range are bound in the antinodes of optical standing waves, thus forming regular microscopic lattices [1–3]. A particularly exciting perspective of optical lattices is the accomplishment of atomic densities where the number of trapped atoms exceeds the number of lattice sites (so far typically 5% of the lattice sites are occupied by an atom). In this regime the lattice should acquire some solid state aspects, and quantum statistics should play an important role for the system dynamics. The realization of microkelvin cold atomic samples with such high densities is certainly one of the most challenging future tasks in laser cooling.

Such hopes, however, are discouraged by the fact that the atomic density in near resonant optical fields is limited to the  $10^{11}$  atoms/cm<sup>3</sup> level, as is well known, e.g., in case of the magneto-optical trap (MOT). This has also limited the atomic densities obtained in optical lattices because of inefficient loading (which so far has in all experiments involved a MOT) and at the same time because of the lattice itself. More efficient loading may be obtained by the combination of multiple loading and refined magneto-optic trapping techniques [4], while the latter problem appears to be more fundamental. Different physical processes are responsible for these limitations which all have in common that coupling the atoms to the light field modifies the light field in a way that disturbs the trapping and cooling mechanisms [5]. As a consequence, atomic densities exceeding a few  $10^{11}$  atoms/cm<sup>3</sup> appear hard to reach in conventional optical lattices.

This has inspired research on new laser cooling and trapping schemes in which the fluorescence of the trapped atoms is strongly suppressed. In the absence of fluorescence the usual light-induced atom-atom interactions [5] are also expected to be suppressed. This may allow studies of novel atom-atom interactions which have not yet been considered. Moreover, in combination with appropriate loading techniques it may allow one to produce

dense optical lattices in the future (which one might call optical crystals).

A one-dimensional (1D) example of a “dark” optical lattice has been theoretically discussed recently by Grynberg and Courtois [6]. In this Letter, we propose and experimentally demonstrate a novel scheme for a 2D dark lattice which can also be extended to 3D. Consider an atom with an  $F = 1 \rightarrow F = 1$  transition ( $F$  is the total angular momentum), and a homogeneous magnetic field oriented along the  $z$  axis which defines our quantization axis. Assume a light field composed of two polarization components; one component  $\mathbf{E}_\pi$  with field vector parallel to the  $z$  axis (which we call  $\pi$  component) and the other component  $\mathbf{E}_\sigma$  with field vector perpendicular to the  $z$  axis (called  $\sigma$  component), such that the nodes of  $\mathbf{E}_\pi$  coincide with the antinodes of  $\mathbf{E}_\sigma$  and vice versa. For blue detuning of the light field with respect to the atomic resonance frequency, atoms are trapped in the nodes of  $\mathbf{E}_\pi$  or  $\mathbf{E}_\sigma$  depending on their magnetic quantum number. Although the total intensity at these locations may be large, the atoms interact only weakly with the light field, because they are optically pumped into an internal state that decouples from the prevailing polarization component.

Let us be more specific in the case of a simple 1D example realized by combining a  $\text{lin} \perp \text{lin}$  standing wave  $(\hat{\mathbf{x}} + \hat{\mathbf{z}})e^{iky} + (\hat{\mathbf{x}} - \hat{\mathbf{z}})e^{-iky}$  along the  $y$  axis with a magnetic field parallel to the  $z$  direction (i.e., perpendicular to the standing wave axis). This light field is the sum of  $\mathbf{E}_\sigma = E_0 \hat{\mathbf{x}} \cos(ky)$  and  $\mathbf{E}_\pi = E_0 \hat{\mathbf{z}} \sin(ky)$ . In Fig. 1(a) we have plotted the energies and populations expected for the three ground state Zeeman levels. The energy splitting  $\hbar\omega_B$  introduced by the magnetic field is assumed to be significantly larger than the light shifts such that  $m_F$  (the  $z$  component of  $F$ ) approximately remains a good quantum number. The dashed lines denote the energies of the three Zeeman levels when only the magnetic field is present. In the antinodes of the  $\pi$  component clearly all atoms are optically pumped to the  $m_F = 0$  Zeeman level which is not coupled by  $\pi$  light, since the corresponding Clebsch-Gordan coefficient vanishes. Similarly,

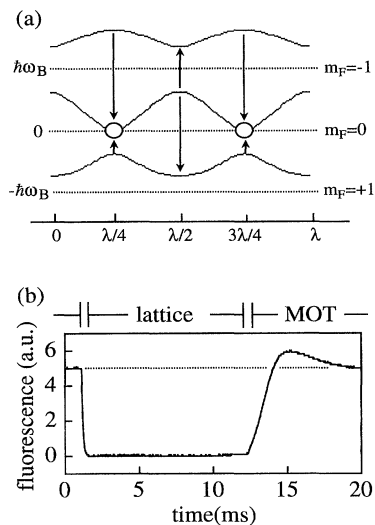


FIG. 1. (a) Schematics of trapping and cooling scheme. (b) Fluorescence of the atomic sample.

in the antinodes of the  $\sigma$  component the population is transferred to the  $m_F = \pm 1$  levels. It is important to note that a noncoupling coherent superposition of  $m_F = \pm 1$  levels (where atomic population would be trapped [7]) does not exist here, because of the magnetic field which lifts the Zeeman degeneracy. If the frequency of the light field is blue detuned with respect to the  $F = 1 \rightarrow F = 1$  transition, optical pumping processes [depicted by the arrows in Fig. 1(a)] tend to transfer the atoms to the least light-shifted levels. The arrows pointing downwards in Fig. 1(a) are always longer than those pointing upwards, indicating that, on average, potential energy is dissipated and the atoms are efficiently cooled. The  $m_F = 0$  atoms are trapped at the nodes of the  $\sigma$  component where they are decoupled from the light field. In the same way, the  $m_F = \pm 1$  atoms are localized at the nodes of the  $\pi$  component where, however, they still interact strongly with the  $\sigma$  component of the light field (the light shift does not vanish at these points). As will be explained in the following, the  $m_F = 0$  trapping potential provides well defined vibrational levels at the bottom which may be resolved by Raman spectroscopy, whereas the  $m_F = \pm 1$  potentials should not give rise to a discrete vibrational structure.

We are now prepared for a 2D extension. Consider the two standing waves  $\mathbf{E}_\sigma = \sqrt{2}E_0 [\hat{x} \cos(ky) + \hat{y} \cos(kx)]$  linearly polarized parallel to the  $x$ - $y$  plane, and  $\mathbf{E}_\pi = \sqrt{2}E_0 \hat{z}[\sin(kx) + i \sin(ky)]$  linearly polarized parallel to the  $z$  axis, where  $\hat{x}, \hat{y}, \hat{z}$  denote the unit vectors in  $x$ ,  $y$ , and  $z$  directions and  $k$  is the wave number. The sum  $\mathbf{E} = \mathbf{E}_\sigma + \mathbf{E}_\pi$  can be obtained by superposing a lin $\perp$ lin standing wave  $(\hat{x} + \hat{z})e^{iky} + (\hat{x} - \hat{z})e^{-iky}$  along the  $y$  axis with a  $\sigma^+\sigma^-$  standing wave  $(i\hat{x} + \hat{z})e^{ikx} + (i\hat{x} - \hat{z})e^{-ikx}$  along the  $x$  axis, such that both waves

oscillate out of phase relative to each other (for this case we define the time-phase difference  $\phi$  between both waves to be  $90^\circ$ ). The nodes of the components  $\mathbf{E}_\pi$  and  $\mathbf{E}_\sigma$  (projected onto the  $x$ - $y$  plane) form 2D point lattices shifted with respect to each other by  $\lambda/4$  in the  $x$  and  $y$  directions. Consequently, the sum  $\mathbf{E} = \mathbf{E}_\sigma + \mathbf{E}_\pi$  provides a 2D analog of the 1D situation sketched in Fig. 1(a). Note that the total intensity of this light field is spatially uniform.

We can estimate the energy separation of adjacent vibrational states and their lifetimes at the bottom of the  $m_F = 0$  and  $m_F = \pm 1$  optical potentials. We begin with the  $m_F = 0$  level in the vicinity of the nodes of  $\mathbf{E}_\sigma$ . The atoms are interacting only weakly with the light field, and we can approximate the light shift  $S_0$  of the  $m_F = 0$  level by its weak coupling expression  $S_0 = \omega_{\max}^2 [\cos(ky)^2 + \cos(kx)^2]/16\delta$ , where  $\omega_{\max}$  is the antinode Rabi frequency. We expand this expression around  $x = y = \pi/2$  yielding  $S_0 \approx \omega_{\max}^2 k^2 (x^2 + y^2)/16\delta$ . The quantum theory of the harmonic oscillator then tells us that the angular frequency of the vibration is  $\omega_{V,0}^2 = \omega_R \omega_{\max}^2 / 4\delta$ , where  $\hbar\omega_R$  is the energy of one photon recoil. In the same way, we may proceed for the  $m_F = \pm 1$  atoms which are trapped at the nodes of  $\mathbf{E}_\pi$ , if we assume low saturation which is sufficiently well fulfilled in the regime of large detunings (i.e.,  $\delta^2 \gg \omega_{\max}^2$ ). The  $m_F = \pm 1$  potentials expanded in the vicinity of  $x = y = 0$  are thus given by  $S_{\pm 1} = S_0/2$  which yields  $\omega_{V,\pm 1} = \omega_{V,0}/\sqrt{2}$ .

Let us estimate the depopulation rates of a given vibrational level in the 2D lattice by similar considerations as presented in Ref. [8]. For the  $m_F = 0$  potential, optical pumping processes leading back to the initial vibrational level without changing the value of  $m_F$  are not possible, because the coupling field  $\mathbf{E}_\sigma$  has odd parity with respect to a nodal point. This is in contrast to the case of conventional optical lattices, where elastic processes exceed all other processes by more than an order of magnitude [9]. Actually, it is the high rate of such elastic processes in conventional optical lattices which should be responsible for the atomic density limitations. The depopulation rates due to transitions changing the value of  $m_F$  have the same magnitude as those resulting from transitions which lead back to the initial  $m_F = 0$  potential. This is also in contrast to conventional lattices where  $m_F$ -conserving transitions play the dominant role in the relaxation of vibrational populations. We find that the inverse lifetimes  $\Gamma_{n,0}$  of vibrational states at the bottom of the  $m_F = 0$  potential can be estimated by the relation  $\Gamma_{n,0} \approx (n+1)\Gamma'/2$ , where  $\Gamma' = s_{\max}\Gamma$  [ $s_{\max} = \omega_{\max}^2/(2\delta^2 + \Gamma^2/2)$ ,  $\Gamma$  is the inverse lifetime of excited state] and  $n = n_x + n_y$  is the sum of the vibrational quantum numbers in a Cartesian reference frame. The small parameter  $\gamma = \omega_R/\omega_{V,0}$  is the square of the so-called Lamb-Dicke factor (for the  $m_F = 0$  potential) which describes the degree of localization of the atom. In our experiment

$\gamma$  is about  $1/23$ . In contrast to this, the depopulation rates  $\Gamma_{n,\pm 1}$  of vibrational levels inside the  $m_F = \pm 1$  potentials are much larger because transitions exchanging population between  $m_F = -1$  and  $m_F = 1$  take place at a much higher rate determined by the intensity of the  $\sigma$  component which has its maximum there. Therefore, we find that  $\Gamma_{n,\pm 1} \approx \Gamma'[1/8 + (n+1)\gamma/\sqrt{2}]$ .

In our experiment we use the rubidium isotope  $^{87}\text{Rb}$  which provides two ground state hyperfine levels  $5S_{1/2}: F = 1, 2$  separated by 6.8 GHz and (795 nm away) two excited state hyperfine levels  $5P_{1/2}: F = 1, 2$  separated by 812 MHz. The experiment proceeds in two steps. During a first phase, a cold sample of atoms (1 mm diameter,  $10^8$  atoms) is prepared with a conventional MOT operating on the  $5S_{1/2}: F = 2 \rightarrow 5P_{3/2}: F = 3$  transition (near 780 nm). The MOT consists of three mutually orthogonal pairs of counterpropagating laser beams with opposite circular polarizations and a quadrupole magnetic field. In order to provide a closed excitation cycle, an additional laser beam is tuned to the  $5S_{1/2}: F = 1 \rightarrow 5P_{3/2}: F = 2$  transition (near 780 nm). The MOT is active for about 50 ms. Then, the repumping beam is disrupted by means of a mechanical shutter, the frequency of the MOT beams is rapidly detuned to a value of a few  $\Gamma$  above the  $5S_{1/2}: F = 2 \rightarrow 5P_{3/2}: F = 2$  resonance (in order to obtain blue detuned optical molasses), and the quadrupole magnetic field is replaced by a homogeneous field parallel to the  $z$  axis. The strength of the magnetic field is 7 G which yields a Larmor frequency  $\omega_B$  of about  $-0.8\Gamma$ . (Note that the Landé factor of the  $F = 1$  ground state is negative. Therefore, the role of the  $m_F = \pm 1$  levels is interchanged in Fig. 1.) The second phase lasts about 10 ms before we return to the MOT phase. During both time periods, the lattice field discussed in the previous paragraphs is present (oriented parallel to the  $x$ - $y$  plane) with an antinode Rabi frequency  $\omega_{\max} = 3.6\Gamma$  for the 2D case (for 1D,  $\omega_{\max} = 2.5\Gamma$ ) and a frequency detuning of  $10\Gamma$  to the blue side of the  $5S_{1/2}: F = 1 \rightarrow 5P_{1/2}: F = 1$  resonance.

In Fig. 1(b) we show the fluorescence emerging from the atomic sample. We see that the fluorescence decreases by a factor of more than 100 during the lattice phase, indicating that the atoms hide in dark states. In order to test the populations in the  $5S_{1/2}: F = 1$  and  $5S_{1/2}: F = 2$  states we have observed the resonant absorption on the  $5S_{1/2}: F = 1, 2 \rightarrow 5P_{1/2}: F = 1, 2$  transitions (which display the same line strength) during the lattice phase finding an absorption ratio of 3:1 and an atomic density of a few times  $10^{11}/\text{cm}^3$ . When the MOT is reactivated, the fluorescence reappears at an intensity exceeding the steady state value in the MOT. (The 2 ms period for switching on the MOT is determined by the mechanical shutter.) When the lattice field is disabled, the fluorescence drops to zero (the entire population is optically pumped to the  $5S_{1/2}: F = 1$  state); however, it takes more than 10 ms to recover when the MOT is switched on and

never exceeds the dotted line in Fig. 1(b). According to these observations the entire atomic population captured by the MOT is indeed preserved by the lattice. The enhanced fluorescence might even indicate an increase of the number of atoms in the dark lattice over that prepared by the MOT which may occur without an increase of the atomic density because the dark lattice extends over a much larger volume (about  $200 \text{ mm}^3$ ) than the atomic sample captured by the MOT. In our present experiment we naturally cannot expect to load atomic samples into the dark lattice at higher densities than achieved with the MOT itself. A possible way to achieve this goal may be the combination of a dark lattice with a strongly off-resonant optical dipole trap and the use of improved magneto-optic loading techniques [4].

A weak probe beam is sent through the atomic sample within the  $x$ - $y$  plane, enclosing a small angle of  $5.7^\circ$  with the  $y$  axis. We employ two independent diode laser (emitting near 795 nm) for the probe beam and the lattice field. To ensure high relative frequency stability, we use phase-locking techniques [10]. The transmitted intensity of the probe laser is recorded versus its detuning from the frequency of the lattice field. The probe scan is started 1.5 ms after the beginning of the second phase and lasts for 5 ms. In Figs. 2(a) and 2(b) we show probe transmission spectra for both the 1D and the 2D lattice discussed in the third and fourth paragraphs, respectively.

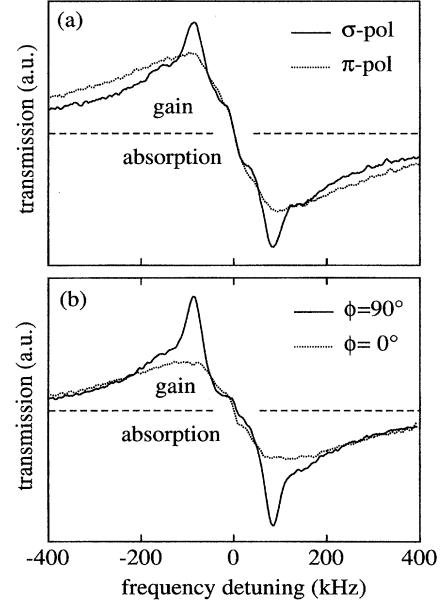


FIG. 2. Probe transmission spectra of dark optical lattices. (a) Spectrum of 1D lattice for  $\sigma$ -polarized probe beam (solid trace) and  $\pi$ -polarized probe beam (dotted trace). ( $\omega_{\max} = 2.5\Gamma$ ,  $\delta = 10\Gamma$ ,  $\omega_B = -0.8\Gamma$ .) (b) Spectrum of 2D lattice for  $\phi = 90^\circ$  (solid trace) and  $\phi = 0^\circ$  (dotted trace). The linear probe polarization was oriented parallel with respect to the nearly copropagating pump beam ( $\omega_{\max} = 3.6\Gamma$ ,  $\delta = 10\Gamma$ ,  $\omega_B = -0.8\Gamma$ ).

Let us begin with the 1D lattice which is realized by a  $\text{lin} \perp \text{lin}$  standing wave along the  $y$  axis. The solid trace in Fig. 2(a) is observed when the probe polarization is oriented perpendicular to the magnetic field, i.e., for  $\sigma$  polarization. In this case only the  $m_F = 0$  potential is time modulated by the interference between the probe beam and the lattice field. Thus, we can excite Raman transitions between different vibrational levels similarly as for conventional optical lattices [1,2,4], giving rise to narrow resonances at  $\pm 85$  kHz. The dotted curve is obtained for  $\pi$  polarization, i.e., when only the  $m_F = \pm 1$  potentials are effected by the probe. If we add the  $\sigma^+ \sigma^-$  standing wave along the  $x$  axis (at  $\phi = 90^\circ$ ) and adjust the probe polarization to be parallel with respect to the nearly copropagating pump wave, we observe the solid trace of Fig. 2(b). We recognize Raman sidebands at the same frequencies, however, slightly narrower than in the 1D case. When the probe polarization is parallel with respect to the nearly counterpropagating pump wave, we do not observe any vibrational structure in the spectrum. The dotted trace in Fig. 2(b) shows the case when  $\phi = 0^\circ$ , which gives rise to a light field that is not appropriate for a 2D optical lattice. Note that one also observes resonances resulting from Raman transitions exchanging two vibrational quanta at about  $\pm 160$  kHz.

The 2D spectrum in Fig. 2(b) corresponds to  $\omega_{\text{max}} = 3.6\Gamma$  and  $\delta = 10\Gamma$  which we have determined with 5% accuracy. Our simple model then predicts  $\omega_{V,0}/2\pi \approx 87$  kHz, which agrees well with the observed value of 8.5 kHz. This indicates that the vibrational structure observed in Fig. 2(b) indeed results from atoms trapped in low lying vibrational levels of the  $m_F = 0$  potential. The fundamental vibrational frequency in the  $m_F = \pm 1$  potentials is a factor of  $\sqrt{2}$  smaller, i.e.,  $\omega_{V,\pm 1}/2\pi \approx 62$  kHz. We also find  $\Gamma_{n,0}/2\pi \approx (n + 1)$  (8.7 kHz) and  $\Gamma_{n,\pm 1}/2\pi \approx (n + 1)$  (12.3 kHz + 49 kHz), showing that only in the case of the  $m_F = 0$  potential may we expect to resolve vibrational sidebands. The observed widths ( $\approx 40$  kHz) of the first sidebands are slightly larger than  $(\Gamma_{1,0} + \Gamma_{0,0})/2\pi = 26$  kHz which results from transitions starting from higher lying vibrational levels. We have modeled the first sideband resonances by taking into account transitions starting from the first five vibrational levels ( $n = 0, 1, 2, 3, 4$ ) in a 2D harmonic potential assuming a thermal distribution of populations and using the relaxation rates  $\Gamma_{n,0}$ . We have used this model to fit the solid trace in Fig. 2(b) between  $\pm 110$  kHz. The only free parameter in this simple model is the temperature yielding  $T = 8 \mu\text{K}$ . A more careful determination of the temper-

ature will be subject to forthcoming experiments. Note, however, that a refinement of our model (e.g., by taking into account anharmonicity effects) would lead to even lower values for the temperature.

The magnetic field strength for the spectra in Fig. 2 corresponds to a Larmor frequency of  $\omega_B = -0.8\Gamma$  which is about twice the antinode light shift of the  $m_F = 0$  level. For Larmor frequencies below  $0.2\Gamma$  the positive light shift of the  $m_F = 1$  level becomes comparable with its negative Zeeman shift, yielding a strong mixing with the  $m_F = 0$  level which disturbs the trapping mechanism. The vibrational structure is completely washed out in this case. When the Larmor frequency approaches the value of the detuning  $\delta$ , the cooling mechanism begins to degrade and again we observe washing out of the vibrational spectra.

Finally, we have also extended our experiment to three dimensions by adding a third standing wave along the  $z$  direction, e.g., with circular polarization. Basically, the only difference we observe in the probe transmission spectra is a slight increase of signal, while the shape and widths of the resonances are practically not altered.

- 
- [1] A. Hemmerich and T. Hänsch, Phys. Rev. Lett. **70**, 410 (1993); A. Hemmerich, C. Zimmermann, and T. Hänsch, Europhys. Lett. **22**, 89 (1993).
  - [2] G. Grynberg, B. Lounis, P. Verkerk, J. Courtois, and C. Salomon, Phys. Rev. Lett. **70**, 2249 (1993).
  - [3] A survey of optical lattices can be found in M. G. Prentiss, Science **260**, 1078 (1993); G. P. Collins Physics Today **46**, 17 (1993).
  - [4] E. Cornell, C. Monroe, and C. Wieman, Phys. Rev. Lett. **67**, 2439 (1991); W. Ketterle, K. Davis, M. Joffe, A. Martin, and D. Pritchard, *ibid.* **70**, 2253 (1993).
  - [5] J. Dalibard, Opt. Commun. **68**, 203 (1988); T. Walker, D. Sesko, and C. Wieman, Phys. Rev. Lett. **64**, 408 (1990); A. Hemmerich, M. Weidemüller, T. Esslinger, and T. Hänsch, Europhys. Lett. **21**, 445 (1993).
  - [6] G. Grynberg and J. Courtois, Europhys. Lett. **27**, 41 (1994).
  - [7] A. Aspect, E. Arimondo, E. Kaiser, N. Vansteenkiste, and C. Cohen-Tannoudji, Phys. Rev. Lett. **61**, 826 (1988).
  - [8] J. Courtois and G. Grynberg, Phys. Rev. A **46**, 7060 (1992).
  - [9] P. Jessen, C. Gerz, P. Lett, W. Phillips, S. Rolston, R. Spreuw, and C. Westbrook, Phys. Rev. Lett. **69**, 49 (1992).
  - [10] L. Ricci, M. Weidemüller, T. Esslinger, A. Hemmerich, C. Zimmermann, and T. Hänsch, Opt. Commun. (to be published).